

Enhanced drug uptake on application of electroporation in a single-cell model

Nilay Mondal^{1†}, K. S. Yadav^{1*†} and D. C. Dalal^{1†}

^{1*}Department of Mathematics, Indian Institute of Technology Guwahati, Amingaon, Guwahati, 781039, Assam, India.

*Corresponding author(s). E-mail(s): yadav176123004@iitg.ac.in;
Contributing authors: nilay.mondal@iitg.ac.in; durga@iitg.ac.in;

[†]These authors contributed equally to this work.

Abstract

Electroporation method is a useful tool for delivering drugs into various diseased tissues in the human body. As a result of an applied electric field, drug particles enter the intracellular compartment through the temporarily permeabilized cell membrane. Consequently, electroporation method allows better penetration of the drug into the diseased tissue and improves treatment clinically. In this study, a more generalized model of drug transport in a single-cell is proposed. The model is able to capture non-homogeneous drug transport in the cell due to non-uniform cell membrane permeabilization. Several numerical experiments are conducted to understand the effects of electric field and drug permeability on drug uptake into the cell. Through investigation, the appropriate electric field and drug permeability are identified that lead to sufficient drug uptake into the cell. This model can be used by experimentalists to get information prior to conduct any experiment, and it may help reduce the number of actual experiments that might be conducted otherwise.

Keywords: Electroporation, drug delivery, interface method, multiple pulses, permeability.

1 Introduction

In order to cure a disease, one aims to deliver a sufficient amount of drug to the diseased site and into the infected cells. The cell membrane is selective

permeable in the sense that it does not allow all the molecules to pass through it. The permeability of the drug across the cell membrane depends on the properties of the drug as well as on the membrane pores.

Over the years, several methods have been developed for drug delivery. In the advancement of technology, new techniques, such as electroporation, micro-injection, laser, ultrasound are developed [1]. Electroporation has been used widely in *in-vitro* and *in-vivo* models in various applications [2–4]. In electroporation, cell membrane is temporarily destabilized by the application of external electric field. This destabilization occurs due to increment in the transmembrane potential [5]. In the destabilization process, the nano-meter size pores are created in lipid bilayers [6–9]. The transitory and permeabilized states of the cell membrane can be exploited to transport drugs into the intracellular domain.

The physical properties of the tissue, such as cell shape, size and its distribution, as well as the electrical parameters, such as the number of pulses, pulse amplitude, pulse duration and tissue conductivity, influence drug transport into the targeted cells [10, 11]. Cell electroporation is commonly used with short and long duration pulses in various experiments. To avoid cell death, single-cell electroporation that involves an inhomogeneous short-duration low-voltage electric field around the cell surface is generally applied. However, the application of high voltage electric field enhances cell membrane pore density [10, 12].

For drug absorption in electroporated cells, it is vital to focus on the increase in permeability and control of cell death. Granot and Rubinsky [13] proposed a model to investigate drug delivery in a tissue with electroporation. In their study, a mass transfer coefficient in terms of pore density based on the pore creation model [6] has been developed. Goldberg et al. [14] proposed a multiphysics model for ion transport, which is also based on the pore creation model. They presented a mass transport model using the Nernst-Planck equation for transporting various species into cells in their model. Goldberg et al. [15] extended their previous model and described the effects of electric pulses on cisplatin transport across the plasma membrane. The model shows that an electric field induces maximum transmembrane potential at the cell poles where the electrodes are placed.

It is a challenging and difficult task to conduct experimental studies of pulse application and field strength on single cell to improve drug uptake. The detailed investigation to determine appropriate class of drugs that can easily enter the cell in a desired amount is still missing in the literature.

In the present article, a mathematical model is employed to study drug transport into a single-cell by the application of electroporation. The prescribed model is more generalized in comparison to the previous models as the spatial changes in cellular drug uptake at different times are analyzed here. This study presents a rigorous analysis of drug delivery into a diseased cell emphasizing the effects of membrane resealing. Drug transport takes place due to diffusion from the extracellular space to the intracellular one. Transport

across the cell membrane takes place due to passive diffusion, which means that the diffusion takes place due to the concentration gradient and the ability of the cell membrane (permeability) to pass the drug. The drug transport equations are solved using the permeable interface method (PIM) on Cartesian mesh by treating the cell membrane as a sharp interface. Various electrode arrangements are tested to determine the locations of maximum pore formation and to analyze the mass transportation through those locations. The numerical experiments are conducted with various electric fields and multiple pulses for a given electric field are used in electroporation to reduce the resealing effects on drug uptake. From the investigation, a suitable electric field is determined to improve the cellular uptake for a specific drug. The numerical experiments are also conducted with drugs of different permeabilities to select the appropriate drug that can be used for treatment to get the best possible efficacy. The resulted non-uniformity of the pores in the cell membrane owing to the application of electric pulses leads to non-uniform drug distribution in the intracellular space.

2 Model formulation

This study investigates the drug transport through the electro-permeabilized cell membrane. A square domain (Ω) of edge length L is considered, and a single-cell is assumed to be placed at the center of Ω . Structurally, the domain can be viewed as two parts: extracellular space and intracellular space. The spaces are separated by the cell membrane, which is selective permeable and controls the mass exchange between the extracellular and intracellular domains. The schematic diagram is shown in the Fig. 1.

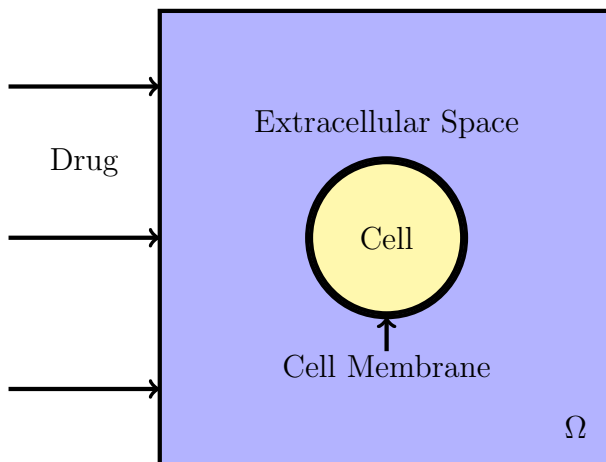


Fig. 1: A schematic diagram of injecting drug into a biological tissue.

4 *Enhanced drug uptake on application of electroporation*

In order to electroporate the cell membrane, two electrodes with potential values ϕ_0 and ϕ_L are placed along the vertical lines at A and B, respectively (as shown in Fig. 2). A uniform electric field E is induced in the region directed from positive to negative electrode. The transmembrane potential (V_m) increases due to the induced electric field. On increasing V_m , cell membrane is destabilized and nanometer-sized pores are generated in the cell membrane as a result of pulse application. Pulses are applied repeatedly for a short duration (1 ms) with maintaining a fixed temporal gap between two pulses. It is assumed that the mass transfer takes place only when the pulse is off. The drug transport from extracellular to the intracellular domain occurs in the resealing period of the cell membrane. The maximum number of pores are created near the poles $\Psi = 0, \pi$, in the setup as shown in Fig. 2, as transmembrane potentials are maximum at those locations; whereas, no new pores are formed at $\Psi = \frac{\pi}{2}, \frac{3\pi}{2}$ as almost negligible transmembrane potential induced at those particular locations.

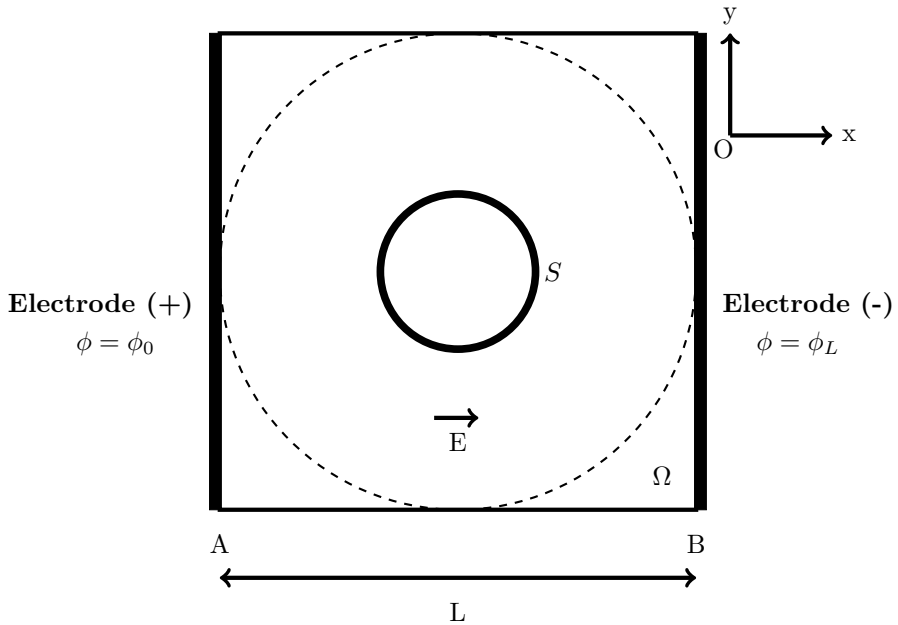


Fig. 2: Schematic representation of a single cell electroporation.

A uniform electric field and non-uniform electric potential has been developed on the arrangement of two parallel electrodes. The potential (ϕ) distribution inside the domain is obtained by solving the Laplace equation given as [9],

$$\nabla^2 \phi = 0. \quad (1)$$

The uniform electric field (E) throughout the domain Ω is obtained by taking the magnitude of potential gradient expressed as,

$$E = |\vec{\nabla}\phi|. \quad (2)$$

2.1 Transmembrane potential and pore calculations

The transmembrane potential (V_m) was initially determined on a spherical cell in a uniform electrical field by Neumann et al. [16]. Later, DeBruin and Krassowska [17] advanced their mathematical model to determine the pore density and its relation with the transmembrane potential. In the present study, we have used the model developed by DeBruin and Krassowska [17] for the investigation of drug delivery into single-cell.

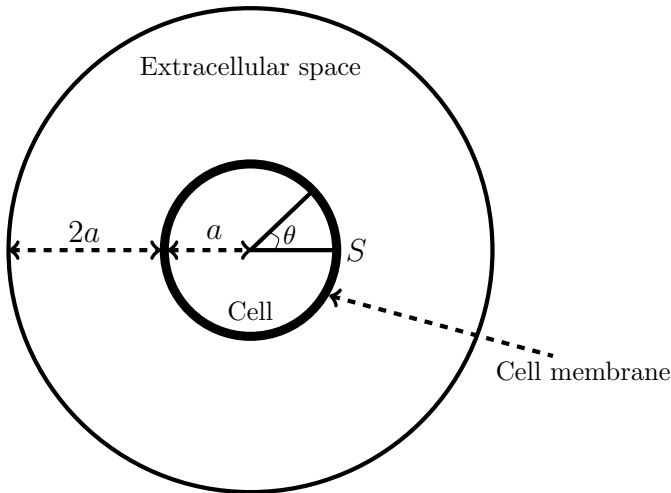


Fig. 3: Schematic diagram of a spherical cell with radius a immersed in extracellular space of thickness $2a$.

We consider a single-cell electroporation in which the spherical cell with radius a is immersed in a spherical shell of extracellular space with radius $3a$. A uniform electric field is induced from the boundary of the extracellular space to destabilize the cell membrane. The physical structure of the model comprising single-cell is schematically portrayed through Fig. 3.

The transmembrane potential V_m on the cell membrane due to the application of electric field is the difference of potentials in intracellular and extracellular domains. As both the domains are source-free, the potentials are calculated using the Laplace equations as [17],

$$\nabla^2\Phi_i = 0 \quad \text{in intracellular space,} \quad (3)$$

$$\nabla^2\Phi_e = 0 \quad \text{in extracellular space,} \quad (4)$$

6 *Enhanced drug uptake on application of electroporation*

where Φ_i and Φ_e are the intracellular and extracellular potentials. The uniform external field E is assumed at the outer boundary and the Φ_e is obtained as,

$$\Phi_e = -3aE \cos \theta. \quad (5)$$

The current density across the cell membrane (S) is given by

$$-\hat{n} \cdot (\sigma_i \nabla \Phi_i) = -\hat{n} \cdot (\sigma_e \nabla \Phi_e) = C_m \frac{\partial V_m}{\partial t} + g_1 (V_m - E_1) + N i_{ep}, \quad (6)$$

where \hat{n} is the unit vector normal to the membrane's surface. σ_i and σ_e are the intracellular and extracellular conductivities, respectively. C_m is the specific membrane capacitance and $V_m = \Phi_i - \Phi_e$ on S . g_1 denotes the specific membrane conductance, t denotes the time and E_1 the reversal potential of the ionic current. The current (i_{ep}) in a single pore is given as [18],

$$i_{ep} = \frac{\pi r_m^2 \sigma v_m RT}{Fh} \frac{e^{v_m - 1}}{\frac{w_0 e^{(w_0 - n v_m)} - n v_m}{w_0 - n v_m} e^{v_m} - \frac{w_0 e^{(w_0 + n v_m)} + n v_m}{w_0 + n v_m}}, \quad (7)$$

where $v_m = V_m \left(\frac{F}{RT} \right)$ is the non-dimensional transmembrane potential.

The pore density $N(t, \theta)$ given by Krassowka and Filev [6] is as follows,

$$\frac{dN}{dt} = \alpha A \left[1 - \frac{N}{N_0} A^{-q} \right], \quad (8)$$

where $A = \exp \left[\left(\frac{V_m}{V_{ep}} \right)^2 \right]$, t the time, α the pore creation rate coefficient, V_m the transmembrane potential, V_{ep} the characteristic voltage of electroporation, N_0 the equilibrium pore density for the membrane area at $V_m = 0$ and q is an electroporation constant. The total number of pores (N_P) in the area Δ_θ of cell membrane after the application of electric pulse (duration is t_{ep}) is obtained as,

$$N_P(\theta) = \oint_{\Delta_\theta} N(t_{ep}) d\theta. \quad (9)$$

2.2 Pore resealing

The pore area decreases with time after electroporation due to the membrane resealing effect, which can be expressed as,

$$A_P(\theta, t) = \pi R_P^2 \cdot N_P(\theta) \exp \left(-\frac{t}{\tau} \right), \quad (10)$$

where τ is the resealing time, Δ_θ is the local area at θ and R_P is the average radius of the pores in the electroporated cell membrane.

The mass transfer coefficient is time dependent and depends on the pore density. The mathematical formulation of the mass transfer coefficient (μ) is given as follows,

$$\mu(\theta, t) = \frac{A_P(\theta, t)}{\Delta_\theta} P, \quad (11)$$

where P is the permeability of drug particles across the cell membrane.

2.3 Drug transport phenomenon in the tissue

The drug concentrations in extracellular space and in the reversibly electroporated cell are obtained by the mass transport equations as,

$$\frac{\partial C_E}{\partial t} = \nabla \cdot (D_E \nabla C_E), \quad (12)$$

$$\frac{\partial C_I}{\partial t} = \nabla \cdot (D_I \nabla C_I), \quad (13)$$

with the initial and boundary conditions

$$C_E(x, y, 0) = \begin{cases} C_0, & x = 0, \\ 0, & \text{otherwise,} \end{cases} \quad (14)$$

$$C_{RE}(x, y, 0) = 0, \quad (15)$$

$$\frac{\partial C_E}{\partial \mathbf{n}} = 0. \quad (16)$$

Here, the subscripts E and I denote the variables from extracellular and intracellular spaces, respectively. C is the drug concentration and D drug diffusivity. C_0 denotes input initial drug concentration. \mathbf{n} is an outward normal vector to the tissue surface.

2.4 Interface conditions

The cell membrane is selective permeable and the permeability depends on the drug properties. The improved permeability of cell membrane (μ) is incorporated in the drug transport as,

$$D_E \nabla C_E = D_I \nabla C_I = \mu(\theta, t)(C_E - C_I)\mathbf{n}. \quad (17)$$

3 Method of solution

The mass transport Eqs. (13)–(17) are solved using the permeable interface method (PIM) proposed by Yadav and Dalal [19]. The PIM can be described briefly as follows. The set of equations are solved using the finite difference method. The domain is discretized using the Cartesian mesh, say the grid point

8 *Enhanced drug uptake on application of electroporation*

is denoted by (i, j) , where i is index in x -direction while j is in the y -direction. The central-difference scheme used to discretize the Eq. (13) is as,

$$(\delta_x (D\delta_x C))_{i,j} + (\delta_y (D\delta_y C))_{i,j} = 0, \quad (18)$$

where

$$(\delta_x (D\delta_x C))_{i,j} = \left\{ \frac{D_{i+1/2,j}C_{i+1,j} - (D_{i+1/2,j} + D_{i-1/2,j})C_{i,j} + D_{i-1/2,j}C_{i-1,j}}{(\delta x)^2} \right\}$$

and

$$(\delta_y (D\delta_y C))_{i,j} = \left\{ \frac{D_{i,j+1/2}C_{i,j+1} - (D_{i,j+1/2} + D_{i,j-1/2})C_{i,j} + D_{i,j-1/2}C_{i,j-1}}{(\delta y)^2} \right\}.$$

Here, the subscript $(i+1/2, j)$ denotes the position $(x_i + \delta x/2, y_j)$ with step-size δx in x -direction. Similarly, other indices are defined.

However, on the grid points near the interface (as depicted in Fig. 4), central-difference scheme can not be used directly. For this, the scheme used is as [20],

$$(\delta_x (D\delta_x C))_i = \left\{ D_{i+\theta/2} \frac{C_{i+\theta}^- - C_i}{x_{i+\theta} - x_i} - D_{i-1/2} \frac{C_i - C_{i-1}}{x_i - x_{i-1}} \right\} / \left(\frac{x_{i+\theta} - x_{i-1}}{2} \right), \quad (19)$$

where $x_{i+\theta} = x_i + \theta\delta x$ for some $0 < \theta < 1$. $C_{i+\theta}^-$ is the limiting concentration at the point $x_{i+\theta}$ approaching from left side (Fig. 4).

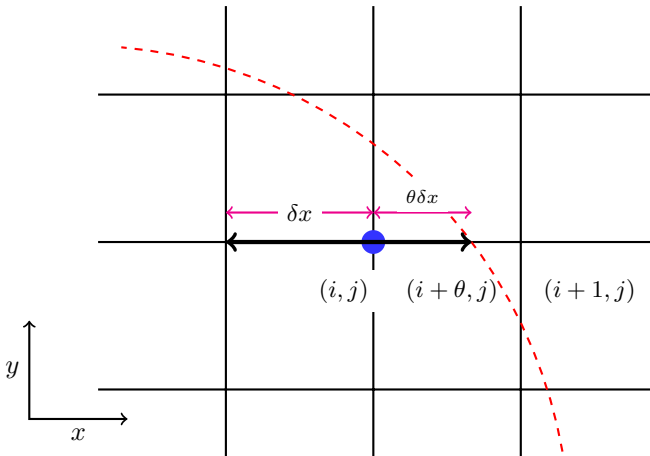


Fig. 4: Discretization near the interface.

The limiting concentrations at the interface are obtained using the linear interpolation from the left and right side, respectively, which also satisfy the interface conditions (Eq. 17) [20]. The resulted system of equations is solved using the BiCGSTAB algorithm without preconditioning with maximum error between two consecutive iterative solutions falls below 10^{-15} .

Table 1: The details of the parameters values used in the simulations.

Sym	Value	Definition	Source
r_c	50 μm	Cell radius	[6]
α	$10^9 \text{ m}^{-2} \text{ s}$	Pore creation coefficient	[6]
V_{ep}	0.258 V	Characteristic voltage	[6]
N_0	$1.5 \times 10^9 \text{ m}^{-2}$	Equilibrium pore density	[6]
q	2.46	Electroporation constant	[13]
D_E	$10^{-3} \text{ mm}^{-2} \text{ s}^{-1}$	Extracellular diffusion coefficient	
D_I	$10^{-4} \text{ mm}^{-2} \text{ s}^{-1}$	Intracellular diffusion coefficient	
R_P	0.8 nm	Pore radius	[13]
P	(0.1 – 1) mm s^{-1}	Permeability of drug	[13]
E	(15 – 40) V mm^{-1}	Electrical field	
C_0	1 M	Initial drug concentration	
L	3 mm	Edge length of the square	Fig. 2
ϕ_0	25 V	Potential at A	Fig. 2
ϕ_L	0 V	Potential at B	Fig. 2
t_{ep}	1 ms	Pulse length (ON TIME)	
t_M	50 s, 100 s	Time for mass transfer (OFF TIME)	
P_N	20	Pulse number	

4 Results and discussion

In this section, the effects of electroporation on drug transport in single-cell are analyzed through numerical experiments. The key parameters, such as drug permeability, electric field and pulse number are explored. In the numerical experiments, repeated pulses with a fixed voltage are applied to make the cell membrane permeabilized and retained this state for a longer period of time. Time gap between any two consecutive pulses is kept to be fixed (50 s or 100 s) for drug transport into the cell. In order to incorporate the physiological situation, the parameters are taken from the literature as listed in the Table 1. The results are obtained on a mesh size 250×250 after ensuring grid independence outcomes.

4.1 Validation

The results obtained from the model are validated with that of Miyauchi et al. [21] and are shown in Fig. 5. For this comparison, a square domain is considered with a cell placed at the center of it as shown in Fig. 5a. $P = 0$ is chosen, so no drug uptake is expected. The concentration distributions along

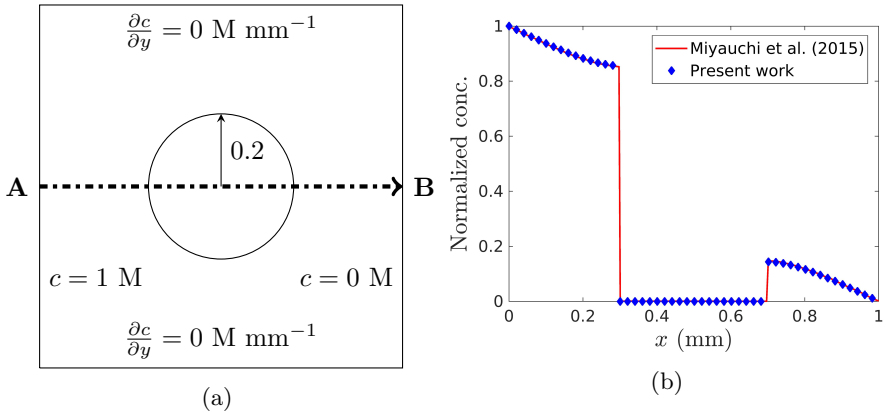


Fig. 5: (a) Computational domain and (b) comparison of present results with the results of Miyauchi et al. [21] along the line **AB** ($y = 0.5$).

the line **AB** are displayed in Fig. 5b. It can be seen that the results are in very good agreement.

4.2 Drug distribution versus time

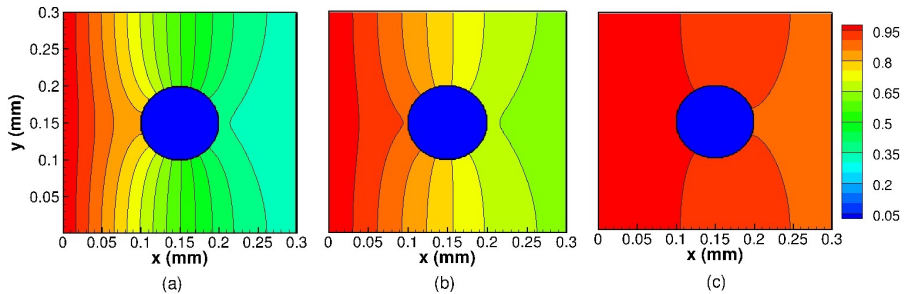


Fig. 6: Contour plots of drug distributions at various times (a) $t = 250$ s, (b) $t = 500$ s and (c) $t = 1000$ s for $P = 0.1$ mm s⁻¹ and $E = 15$ V mm⁻¹.

Fig. 6 shows the contour plots of drug transport into the intracellular space from the extracellular region through the permeabilized cell membrane. It shows drug concentrations for different time durations, as $t = 250$ s, 500 s, and for 1000 s. The drug uptake into the cell is very low due to the application of low voltage (15 V mm⁻¹) pulses. The reason is that when low voltage pulses are applied to the tissue, fewer number of pores are created in the cell membrane, and as a result, the membrane do not get sufficiently permeabilized for drug uptake.

In order to improve membrane permeability, it is necessary to increase the electric field strength (i.e., $E > 15 \text{ V mm}^{-1}$) of the applied pulses in the experiments. Since a high voltage pulse enhances the number of pores and their area in the cell membrane (see Eq. (8)), this gives rise to increase in mass transfer rate. The mass transfer rate may also increase for some drugs (basically small sized pharmaceutical molecules) that are highly permeable to the target cell membrane. This is due to the mass transfer coefficient μ , which is directly proportional to drug permeability P (Eq. (11)). So, several experiments are conducted to analyze the role of field strength of the applied pulses and drug permeability.

4.3 Effects of electric field on drug penetration

The experiments are conducted on the application of 20 pulses of 1 ms with three different electric fields as, $E = 15, 25$ and 40 V mm^{-1} . Fig. 7 shows the effects of electric field on drug uptake. From Figs. 7a, 7b, it can be noticed that the drug uptake is very less due to insufficient permeabilization of the cell membrane with low voltage pulses ($E = 15, 25 \text{ V mm}^{-1}$). So, $E = 15, 25 \text{ V mm}^{-1}$ are not suitable voltages for introducing sufficient drug uptake into the cell. Another experiment for $E = 40 \text{ V mm}^{-1}$ with the same value of drug permeability ($P = 0.1 \text{ mm s}^{-1}$) is conducted to observe the effects of high electric pulse on mass transport into the cell. The results are shown in Fig. 7c. A significant improvement in drug uptake is noticed; thus, sufficiently strong electric field is required in order to permeabilize the cell membrane appropriately. As indicated in Fig. 7c, drugs enter the cell through both the sides ($\theta = 0, \pi$), where maximum pores are created.

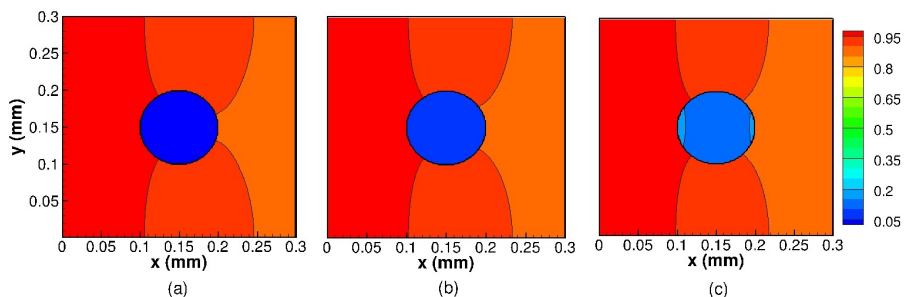


Fig. 7: Effects of electric field (a) $E = 15 \text{ V mm}^{-1}$, (b) $E = 25 \text{ V mm}^{-1}$ and (c) $E = 40 \text{ V mm}^{-1}$ ($P = 0.1 \text{ mm s}^{-1}$, $t = 1000 \text{ s}$).

Fig. 8 shows the concentrations against the time obtained from some selected points inside the cell. The selected points are $(0.11, 0.15)$, $(0.15, 0.15)$ and $(0.19, 0.15)$. Clearly, one can observe that the drug concentration increases with time owing to the drug uptake. Effects of several pulses can be seen. On a given pulse, drug uptake initially improves and then it gets saturated due

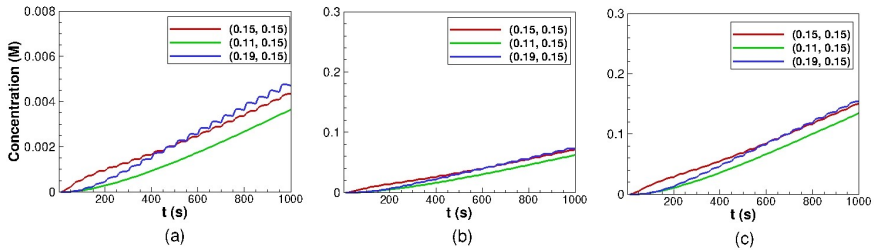


Fig. 8: Concentration vs time inside the intracellular space for (a) $E = 15 \text{ V mm}^{-1}$, (b) $E = 25 \text{ V mm}^{-1}$ and (c) $E = 40 \text{ V mm}^{-1}$ ($P = 0.1 \text{ mm s}^{-1}$).

to the resealing effect, which subsequently requires another shot of pulse for faster uptake. Clearly, the intracellular concentration increases with increasing E . The maximum intracellular concentration is achieved for $E = 40 \text{ V mm}^{-1}$.

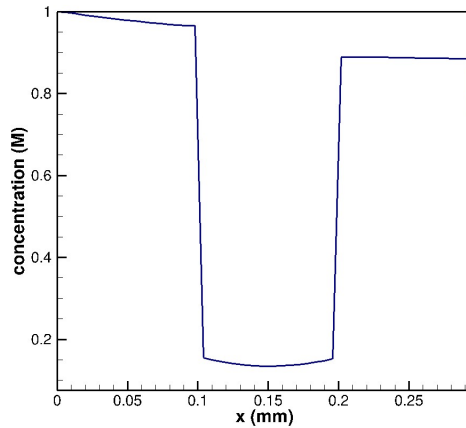


Fig. 9: Concentration across a cross-section of domain at $y = 0.15$ for $P = 0.1 \text{ mm s}^{-1}$ and $E = 40 \text{ V mm}^{-1}$.

Fig. 9 displays the concentration distribution of drug along the line $y = 0.15$ in the tissue domain. The result is obtained at the end of the process in which 20 pulses of 1 ms with maintaining a 50 s temporal gap between the two consecutive pulses are considered. The figure shows that the extracellular concentration of the drug is much higher than the intracellular concentration. The use of a high electric field and the application of repeated pulses improve drug uptake into the cell. Therefore, our goal is to choose the electroporation parameters based on both the properties of a drug as well as the amount of drug that needs to be introduced into the cell.

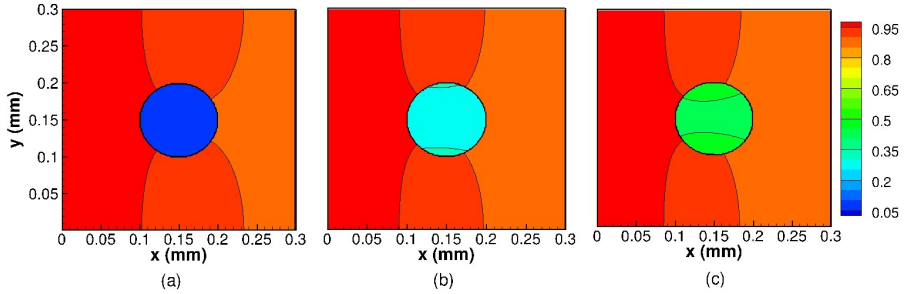


Fig. 10: Effects of drug permeability (a) $P = 0.1 \text{ mm s}^{-1}$, (b) $P = 0.5 \text{ mm s}^{-1}$ and (c) $P = 1 \text{ mm s}^{-1}$ ($E = 25 \text{ V mm}^{-1}$, $t = 1000 \text{ s}$).

4.4 Effects of drug permeability on drug penetration

In order to observe the effects of drug permeability on cellular uptake, numerical experiments are conducted with different permeability values for the voltage $E = 25 \text{ V mm}^{-1}$. The results shown in Fig. 10 explain that the drug uptake increases with the increase in P , as the mass transfer rate increases with P . This shows that the drugs having higher permeability are required when low voltage fields are employed. It is evident from Figs. 10b, c that a large amount of drug ($> 0.2 \text{ M}$) has entered the cell, which may be sufficient to treat the infected cell. Thus, the drugs with permeability greater than 0.005 can be chosen to inject it into the cell for $E = 25 \text{ V mm}^{-1}$.

4.5 Optimal choice of E and P for enhanced drug uptake

Fig. 11 shows the drug penetration into the cell at different times on application of pulses with a suitable voltage ($E = 25 \text{ V mm}^{-1}$) and appropriate choice of drug permeability $P = 0.5 \text{ mm s}^{-1}$. From Fig. 11a, it can be noticed that the drug uptake has started at 250 s from the left side of the cell when a sufficient amount of drug is diffused nearby the cell. On increasing time, the drug spreads out in the extracellular space and enters into the cell. Fig. 11b illustrates that the drug enters into the cell through the pores at $\theta = \pi$ once some drug reach near this location due to the molecular diffusion. At the end of the process of drug delivery ($t = 1000 \text{ s}$), the drug concentration inside the cell is $\approx 0.25 \text{ M}$ by continuous drug uptake through both the left and right sides of the cell, which is shown in Fig. 11c. The significant increase in drug concentration into the cell is obtained due to increased mass transfer rate on a proper choice of electric field and drug permeability.

From the Fig. 12, it can be seen that the cellular drug uptake (for $E = 40 \text{ V mm}^{-1}$ and $P = 0.1 \text{ mm s}^{-1}$) is almost equivalent to the drug uptake for $E = 25 \text{ V mm}^{-1}$ and $P = 0.5 \text{ mm s}^{-1}$ (see Fig. 11). One can notice from Figs. 11c and 12c that the drug concentration into the cell is in the range $0.2 - 0.3 \text{ M}$ for both the cases. Therefore, these parameters' values ($E = 20 \text{ V mm}^{-1}$,

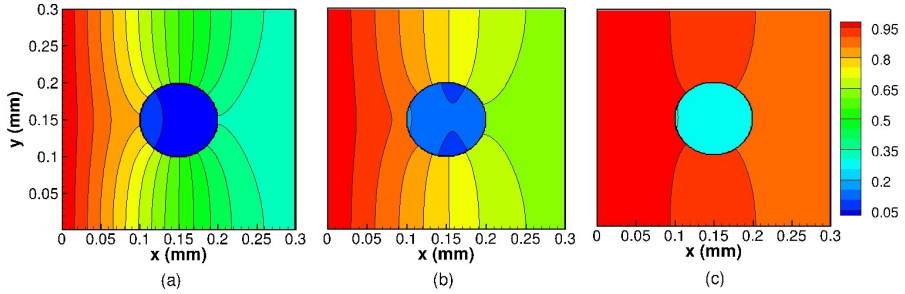


Fig. 11: Contour plots of drug penetration at various times (a) $t = 250$ s, (b) $t = 500$ s and (c) $t = 1000$ s for $P = 0.5$ mm s⁻¹ and $E = 25$ V mm⁻¹.

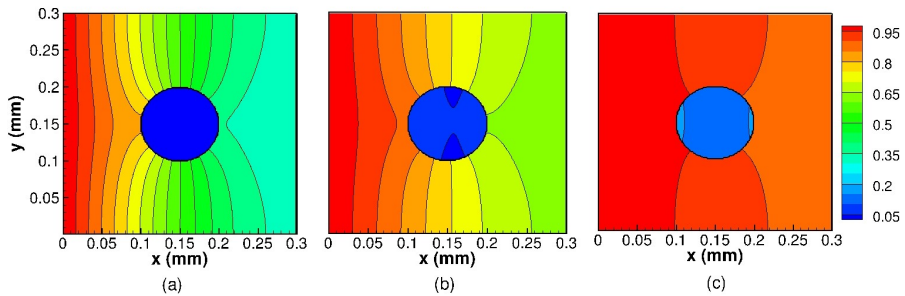


Fig. 12: Contour plots of drug penetration at various times (a) $t = 250$ s, (b) $t = 500$ s and (c) $t = 1000$ s for $P = 0.1$ mm s⁻¹ and $E = 40$ V mm⁻¹.

$P = 0.5$ mm s⁻¹ or $E = 40$ V mm⁻¹, $P = 0.1$ mm s⁻¹) can be taken into the consideration for the treatment of cancer cells by clinical experimentalists.

4.6 Effects of number of pulses

In order to study the effects of pulse shots on drug uptake, numerical experiments are performed in two ways; one, where a pulse is given after each 50 s while in other, a pulse is given after each 100 s. In the latter case, the time between two consecutive pulses is large, and consequently, for a given simulation time period the number of pulses is lesser. Concentration versus time on some intracellular points are plotted in Fig. 13. The drug concentration increases over time for the application of pulses (PN : 20 if pulse gap is 50 s and 10 if pulse gap is 100 s). However, drug uptake improves on increasing the number of pulses. It is due to the resealing effects that will be pronounced if the time gap is more between two consecutive pulse shots.

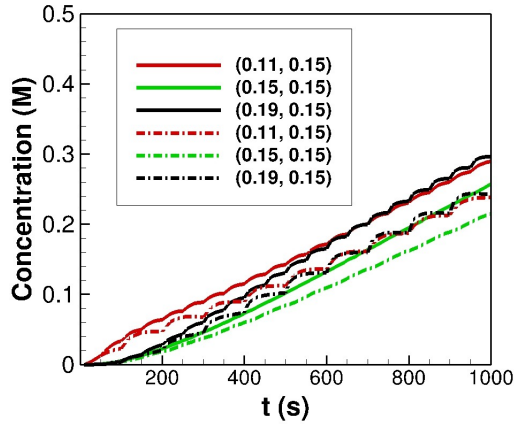


Fig. 13: Effects of number of pulse shots on drug uptake ($E = 25 \text{ V mm}^{-1}$, $P = 0.5 \text{ mm s}^{-1}$). Solid lines ‘—’ show for 50 s pulse gap while dashed lines ‘- -’ represent 100 s pulse gap.

4.7 Arrangement of electrodes

In order to understand the effects of arrangement of electrodes, the experiments are conducted by setting electrodes on the top and bottom of the cell. In this case, the higher pore density is obtained at the top and bottom of the cell, i.e., for $\theta = \frac{\pi}{2}$ and $\frac{3\pi}{2}$. Fig. 14 shows drug distributions for different drug permeability values. In the extracellular region, drug distribution patterns are the same as obtained in earlier cases. However, drug uptake happens from the top and bottom parts of the cell, where pore density is high owing to the particular arrangement of electrodes.

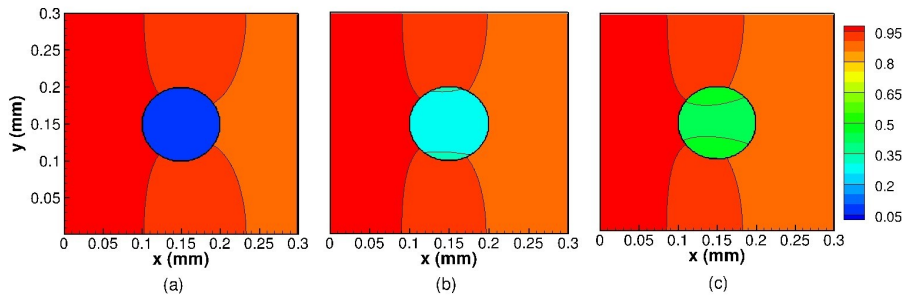


Fig. 14: Drug distribution for the case where electrodes are placed at the top and bottom sides for (a) $P = 0.1 \text{ mm s}^{-1}$, (b) $P = 0.5 \text{ mm s}^{-1}$ and (c) $P = 1 \text{ mm s}^{-1}$ ($E = 25 \text{ V mm}^{-1}$).

5 Conclusions

In this study, drug transport in a single-cell model has been studied. The effects of electroporation on drug uptake into the single-cell are explored. The transport across the cell membrane is incorporated using the permeable interface method available in the literature. Here, an advanced model in the area of electroporation drug delivery is analyzed as it provides the following important outcomes.

Numerical experiments are conducted for electric fields $E = 15, 25$ and 40 V mm^{-1} and for different drug permeabilities. It is noticed that the drug uptake into the cell is almost negligible on the application of significantly low voltage ($E = 15 \text{ V mm}^{-1}$) pulses whereas a significant improvement in drug uptake occurs for $E = 40 \text{ V mm}^{-1}$. A strong electric field is required to permeabilize the cell membrane properly, allowing a desired amount of drug to enter the cell. Based on the numerical experiments on the proposed model, it is learned that the suitable electric field is 25 V mm^{-1} or more, and appropriate drugs whose permeability is at least 0.5 mm s^{-1} for getting a desired amount of drug into the targeted cell. This is a new finding from the prescribed model. Thus, in practice, parameter values ($E = 25 \text{ V mm}^{-1}$, $P = 0.5 \text{ mm s}^{-1}$ or $E = 40 \text{ V mm}^{-1}$, $P = 0.1 \text{ mm s}^{-1}$) can be chosen to deliver pharmaceutical compounds into the targeted cell that needs treatment.

The drug uptake is initiated as soon as the application of pulse is completed. However, the drug uptake slows down due to the resealing effect, another shot of pulse is required to restore the mass transport. So, multiple pulses are required to increase the drug uptake and to achieve the desired level of drug absorption into the cell. The maximum drug uptake occurs through the poles at $\theta = 0, \pi$ on setting electrodes on the left and right sides of the cell. Enhanced drug uptake is obtained for high permeable drugs, high voltage pulses, and by increasing the number of pulses.

Acknowledgments. The first-two authors are financially supported by Indian Institute of Technology Guwahati for conducting this work.

Conflict of interest

On behalf of all authors, the corresponding author states that there is no conflict of interest.

References

- [1] Bolhassani, A., Mohit, E., Ghasemi, N., Salehi, M., Taghikhani, M., Rafati, S.: Enhancement of potent immune responses to HPV16 E7 antigen by using different vaccine modalities. *B. M. C. Proceedings* **5**, 19 (2011)

- [2] Dermol-Černe, J., Miklavčič, D.: From cell to tissue properties—modeling skin electroporation with pore and local transport region formation. *IEEE Transactions on Biomedical Engineering* **65**(2), 458–468 (2018)
- [3] Kotnik, T., Rems, L., Tarek, M., Miklavčič, D.: Membrane electroporation and electropermeabilization: Mechanisms and models. *Annual Review of Biophysics* **48**(1), 63–91 (2019)
- [4] Dermol-Černe, J., Pirc, E., Miklavčič, D.: Mechanistic view of skin electroporation – models and dosimetry for successful applications: an expert review. *Expert Opinion on Drug Delivery* **17**(5), 689–704 (2020)
- [5] Neumann, E., Schaefer, R.M., Wang, Y., Hofschneider, P.H.: Gene transfer into mouse lyoma cells by electroporation in high electric fields. *The EMBO Journal* **1**(7), 841–845 (1982)
- [6] Krassowska, W., Filev, P.D.: Modeling electroporation in a single cell. *Biophysical Journal* **92**(2), 404–417 (2007)
- [7] Mahnič-Kalamiza, S., Vorobiev, E., Miklavčič, D.: Electroporation in food processing and biorefinery. *The Journal of Membrane Biology* **247**, 1279–1304 (2014)
- [8] Napotnik, T.B., Reberšek, M., Vernier, P.T., Mali, B., Miklavčič, D.: Effects of high voltage nanosecond electric pulses on eukaryotic cells (in vitro): A systematic review. *Bioelectrochemistry* **110**, 1–12 (2016)
- [9] Mondal, N., Chakravarty, K., Dalal, D.C.: A mathematical model of drug dynamics in an electroporated tissue. *Mathematical Biosciences and Engineering* **18**(6), 8641–8660 (2021)
- [10] Pavlin, M., Kandu, S.M., Reberšek, M., Pucihar, G., Hart, F.X., Magjarevicacute, R., Miklavčič, D.: Effect of cell electroporation on the conductivity of a cell suspension. *Biophysical Journal* **88**(6), 4378–4390 (2005)
- [11] Pucihar, G., Krmelj, J., Reberšek, M., Napotnik, T.B., Miklavčič, D.: Equivalent pulse parameters for electroporation. *IEEE Transactions on Biomedical Engineering* **58**(11), 3279–3288 (2011)
- [12] Weaver, J.C.: Electroporation of biological membranes from multicellular to nano scales. *IEEE Transactions on Dielectrics and Electrical Insulation* **10**, 754–768 (2003)
- [13] Granot, Y., Rubinsky, B.: Mass transfer model for drug delivery in tissue cells with reversible electroporation. *International Journal of Heat and Mass Transfer* **51**(23), 5610–5616 (2008)

- [14] Goldberg, E., Suárez, C., Alfonso, M., Marchese, J., Soba, A., Marshall, G.: Cell membrane electroporation modeling: A multiphysics approach. *Bioelectrochemistry* **124**, 28–39 (2018)
- [15] Goldberg, E., Soba, A., Gandía, D., Fernández, M.L., Suárez, C.: Coupled mathematical modeling of cisplatin electroporation. *Bioelectrochemistry* **140**, 107788 (2021)
- [16] Neumann, E., Jordan, C.A., Sowers, A.E.: *Electroporation and Electrofusion in Cell Biology*. Springer, Cham (1989)
- [17] DeBruin, K.A., Krassowska, W.: Modeling electroporation in a single cell. i. effects of field strength and rest potential. *Biophysical Journal* **77**(3), 1213–1224 (1999)
- [18] DeBruin, K.A., Krassowska, W.: Electroporation and shock-induced transmembrane potential in a cardiac fiber during defibrillation strength shocks. *Annals of Biomedical Engineering* **26**(4), 584–596 (1998)
- [19] Yadav, K.S., Dalal, D.C.: Effects of cell permeability on distribution and penetration of drug in biological tissues: A multiscale approach. *Applied Mathematical Modelling* **108**, 355–375 (2022)
- [20] Yadav, K.S., Dalal, D.C.: The heterogeneous multiscale method to study particle size and partitioning effects in drug delivery. *Computers and mathematics with applications* **92**, 134–148 (2021)
- [21] Miyachi, S., Takeuchi, S., Kajishima, T.: A numerical method for mass transfer by a thin moving membrane with selective permeabilities. *Journal of Computational Physics*

Statements & Declarations

- The authors declare that no funds, grants, or other support were received during the preparation of this manuscript.
- The authors have no relevant financial or non-financial interests to disclose.
- The authors declare that the results/data/figures in this manuscript have not been published elsewhere, nor are they under consideration by another publisher.
- The datasets generated during and/or analysed during the current study are available from the corresponding author on reasonable request.
- All authors contributed equally to this work.